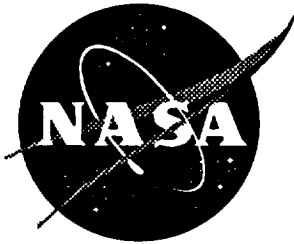


1N-24  
60142

NASA Technical Memorandum 110251



# Fatigue Response of Perforated Titanium for Application in Laminar Flow Control

J. L. Miller and J. C. Newman, Jr.  
*Langley Research Center, Hampton, Virginia*

W. S. Johnson  
*Georgia Institute of Technology, Atlanta, Georgia*

April 1996

National Aeronautics and  
Space Administration  
Langley Research Center  
Hampton, Virginia 23681-0001



# FATIGUE RESPONSE OF PERFORATED TITANIUM FOR APPLICATION IN LAMINAR FLOW CONTROL

Jennifer L. Miller<sup>1</sup>, James C. Newman<sup>2</sup>, Jr. and W. Steven Johnson<sup>3</sup>

**Abstract:** The room temperature tensile and fatigue response of non-perforated and perforated titanium for laminar flow control application was investigated both experimentally and analytically. Results showed that multiple perforations did not affect the tensile response, but did reduce the fatigue life. A two dimensional finite element stress analysis was used to determine that the stress fields from adjacent perforations did not influence one another. The stress fields around the holes did not overlap one another, allowing the material to be modeled as a plate with a center hole. Fatigue life was predicted using an equivalent initial flaw size approach to relate the experimental results to microstructural features of the titanium. Predictions using flaw sizes ranging from 1 to 15  $\mu\text{m}$  correlated within a factor of 2 with the experimental results by using a flow stress of 260 MPa. By using two different flow stresses in the crack closure model and correcting for plasticity, the experimental results were bounded by the predictions for high applied stresses. Further analysis of the complex geometry of the perforations and the local material chemistry is needed to further understand the fatigue behavior of the perforated titanium.

**KEY WORDS:** commercially pure titanium, tensile response, fatigue crack growth, life prediction, cracks.

---

<sup>1</sup>Resident Research Associate, NASA Langley Research Center, MS 188E, Hampton, VA.

<sup>2</sup>Senior Scientist, NASA Langley Research Center, MS 188E, Hampton, VA.

<sup>3</sup>Professor of Materials Science and Engineering, Georgia Institute of Technology, Atlanta, GA.

Laminar flow control has been shown to significantly improve the aerodynamic efficiency of aircraft by stabilizing the boundary layer along wing surfaces, thereby reducing drag [1]. The benefits of this improvement are increased cargo capacity, longer flight range, and lower fuel consumption. These are critical issues for developing a cost effective commercial aircraft particularly for hypersonic applications. One method of achieving laminar flow proposes reducing the boundary layer along the wing surface by applying suction through a multitude of very small holes in the wing skin [2]. Although the perforations are minuscule, the enormous number of perforations required to achieve laminar flow would greatly reduce the net section area of the wing and could present possible structural problems. It was of interest to examine the effect of these perforations on the mechanical properties of the material, particularly in regard to effects on fatigue life.

The objectives of this study were to investigate the influence of multiple perforations on the fatigue behavior of commercially pure titanium and to predict the fatigue life of the perforated material by using an elastic-plastic crack closure model. The experimental study included room temperature tension tests to characterize the material's mechanical properties and room temperature constant amplitude fatigue tests. To establish a baseline for comparison, non-perforated sheets were also tested in tension and fatigue. A two dimensional finite element analysis was used to determine whether the stress fields from adjacent perforations influenced one another. From the stress analysis the geometry for the life prediction model was established. Fatigue crack growth tests were conducted to provide input to the crack closure model. Life predictions were made using an equivalent initial flaw size approach to relate the experimental constant amplitude fatigue results to the microstructural features of the titanium.

### **Material and Specimen Geometry**

The sheet material used in this investigation was commercially pure titanium of 0.91 mm nominal thickness. The chemical composition is shown in Table 1. Optical microscopy revealed acicular alpha present within the alpha grains (Figure 1), indicating that the titanium had been annealed above the beta transus temperature of approximately 915° C [3]. The average grain size

was determined from the average linear intercept method to be 15  $\mu\text{m}$ . No further heat treatment was applied to the material.

Both non-perforated and perforated titanium sheets were received. The perforations were made by laser drilling the holes in a periodic array. Figure 2 displays the two surfaces of the perforated sheet. The perforations are conical in shape, resulting in the two different surface hole diameters as shown in the photographs and the schematic diagram of Figure 2. The irregularity of the edges of the holes and the conical shape result from the laser drilling process. Throughout the analysis the holes were treated as right circular cylinders, with an average hole diameter of 0.12 mm. The average center-to-center hole spacing of the holes in the crack growth direction was 1.2 mm and the average number of perforations across the 19 mm gage width of the test specimens perpendicular to the load direction was 11.

Room temperature tension tests were conducted on the perforated and non-perforated sheets using 150 mm long dog bone specimens with a 50 mm long by 19 mm wide gage length. The fillet radius was 25 mm. Dog bone specimens were also used for fatigue testing the non-perforated material. Straight sided specimens, 150 mm long and 19 mm wide, were used to test the perforated sheet in fatigue since early tests on dog bone specimens resulted in crack growth in the fillet section where the perforations were cut through during specimen manufacturing. The straight sided specimens were machined to avoid having cut holes along the specimen edges. Non-perforated center-cracked specimens, 150 mm long and 50 mm wide, were used for fatigue crack growth tests. Electronic discharge machining was used to produce the 1.3 mm by 0.25 mm central slot. After machining, all specimens were degreased and cleaned ultrasonically in distilled water to remove any particles from within the holes. The center cracked specimens were polished on one surface to a 0.1  $\mu\text{m}$  finish to aid in monitoring crack growth.

### **Experimental Procedure**

The tensile specimens were tested monotonically to failure at a loading rate of 8900 N/min at room temperature. Axial strain measurements were made using a strain-gage extensometer with a 25 mm gage section. Results were recorded on an X-Y plotter.

Room temperature constant amplitude fatigue tests were conducted in load control at an R-ratio of 0.1 and a frequency of 10 Hz for various applied load levels (150 to 300 MPa). Periodically the fatigue test was interrupted to measure the material's modulus. A single load cycle was applied at a slower loading rate of 4500 N/min. The results were recorded on an X-Y plotter. The test continued until the specimen failed.

Fatigue crack growth experiments were conducted in accordance with ASTM standard E647 [4]. Room temperature constant amplitude fatigue crack growth tests were conducted in load control at R-ratios of 0.1 and 0.5, at a frequency of 10 Hz. An additional K-decreasing test was conducted at R=0.1 and 10 Hz. The maximum stress levels for the R=0.1 tests were 124 MPa and the R=0.5 was 172 MPa. Crack growth measurements were made at increments of 0.25 mm during all tests.

### **Analytical Methods**

The two dimensional finite element analysis code, FRANC 2D [5], was used to analyze the stress fields around adjacent perforations to determine the whether the stress fields from the holes interact. As a comparison, an infinite plate with a central hole was also analyzed. Details of this analysis are found in Appendix A.

The life prediction model, FASTRAN-II [6], was used to predict the fatigue life of the perforated titanium. The model accounts for plasticity induced crack closure when calculating the crack-tip opening stress level and the corresponding effective stress intensity factor. The crack length is adjusted by adding a portion of the cyclic plastic zone to correct for plasticity in the stress intensity factor solution. A detailed description of the model is found in reference 6.

In analyzing the perforated titanium, an approximate solution for two corner-cracks propagating from a central hole was made by adjusting the boundary correction factor for through-cracks propagating from a central hole. Figure 3 is a schematic diagram of the corner-crack and through-crack configurations. The stress intensity factor solution for through-cracks growing from a central hole is

$$K_{TC} = S\sqrt{\pi c} F\left(\frac{c}{r}\right) \quad (1)$$

where  $S$  is the applied stress,  $c$  is the crack length,  $r$  is the hole radius and  $F$  is the boundary correction factor. The corner-crack stress-intensity factor solution in FASTRAN did not cover the hole diameter-to-thickness ratio used in the test specimens. To approximate the corner-crack solution, the ratio of the stress intensity factors for a through-crack at a central hole ( $K_{TC}$ ) and a corner-crack in a bar ( $K_{CC}$ ) was determined for a given initial crack length

$$\zeta = \frac{K_{CC}}{K_{TC}} \quad (2)$$

The shape of the crack was assumed to be a quarter-circle. The boundary correction factor was then reduced by this factor,  $\zeta$ , in the through-crack solution to account for the increased life due to the crack growth from smaller initial corner-cracks.

Since commercially pure titanium plastically deforms at relatively low stress levels, two different flow stresses were used for the life predictions. The flow stress is defined as the average of the yield stress and the ultimate strength of the material [6]. Typically the 0.2% offset yield stress is used; however, due to the highly ductile nature of the titanium, both the proportional limit stress and the 0.2% offset yield stress were used to calculate two flow stresses. This allowed upper and lower bounds to be established on the fatigue life predictions for given initial flaw sizes.

## Results and Discussion

The typical room temperature tensile results for the non-perforated and perforated titanium are shown in terms of the net section stress in Figure 4. The net section stress was calculated assuming there was an average of 11 perforations across the width of the specimen. Table 2 shows the mechanical properties determined from these tests. For the perforated titanium, the ratio of the gross elastic modulus to the net elastic modulus is equal to the average volume fraction of

holes, 10%. There is less than 5% difference in mechanical properties between the two materials indicating that the holes do not affect the tensile response of the material.

Figure 5 presents the results from constant amplitude fatigue tests at room temperature on the non-perforated and perforated titanium in terms of maximum applied (gross) stress. The perforated titanium showed much shorter fatigue lives at every stress level tested. When the fatigue life is shown as a function of net section stress, as shown in Figure 6, life is reduced by an order of magnitude at stress levels below 290 MPa (260 MPa applied stress). If the elastic stress concentration effect at hole (assumed to be  $K_t=3$ ) was acting alone to reduce the fatigue life, the stress near the hole would be higher than the ultimate strength of the material even at the lowest applied stress level. Fatigue experiments suggest that notches produce less of a stress concentration effect than would be expected from the theoretical elastic stress concentration factors for the notch geometry [7]. The reduced life shown by the perforated titanium can be viewed as a measure of the notch sensitivity of the material.

After fatigue testing, the surfaces of the perforated titanium specimens were microscopically inspected for fatigue cracks. Depending on the stress level, the surfaces appeared very different, as seen in Figure 7. At the lower stress levels, below 260 MPa applied stress, numerous small cracks were seen throughout the gage section of the specimen growing from the perforations. The cracks do not seem to influence one another since they appear to grow along a relatively straight path. At stress levels higher than 260 MPa, the amount of plastic deformation increases and local yielding occurs near the holes, as shown in Figure 7b. These differences in crack growth behavior also correspond to the differences in the measured reduction in elastic modulus during fatigue cycling. Figure 8 displays the reduction in elastic modulus for two different applied stress levels, 276 MPa and 186 MPa, respectively. At 276 MPa plastic deformation occurred throughout the test and the modulus decreased rapidly as plastic strain accumulated. At the lower stress level very little plastic deformation was seen prior to final net section yielding, but many small cracks were found at the holes along the gage section. The modulus decreased much less than at the higher stress level until final failure occurred by net

section yielding. At the lower stress level the reduction in modulus was attributed to the growth of many small cracks rather than extensive plastic deformation that occurs at higher stresses.

Fatigue crack growth tests were conducted to characterize the fatigue crack growth behavior of commercially pure titanium at  $R=0.1$  and  $0.5$  for input into the FASTRAN-II model. The results of these tests are shown in Figure 9. To correct for plasticity induced crack closure, the crack opening stress equations for constant amplitude loading were used [8] and the plastic zone correction was applied to determine the effective plastic stress intensity factor. Because the test data fell above the stress intensity factor that corresponds to the flat-to-slant transition (approximately  $4 \text{ MPa}\sqrt{\text{m}}$ ), a low constraint factor,  $\alpha=1.2$  was chosen in the closure correction. A previous study on titanium alloys showed that this constraint factor was appropriate above the transition region [9]. Figure 10 shows the results of the fatigue crack growth tests when the stress intensity factor range is corrected for crack closure for both R-ratios. A multi-linear curve fit (solid line) was used to describe the crack growth data for FASTRAN-II predictions. Verification of the average curve fit data conducted for the center-cracked specimen under the experimental loading conditions gave crack growth predictions within  $\pm 25\%$  of the experimental results. The baseline crack growth curve was used to further predict the fatigue life of the perforated titanium using a center-hole specimen geometry.

Fatigue life predictions were made for the perforated titanium with a variety of initial flaw sizes, consistent with the microstructure of the material. As previously shown, the microstructure consisted primarily of equiaxed alpha grains with some acicular alpha imbedded in the grains. The flaws sizes chosen corresponded to the alpha needle width, needle length and the average grain size. Figure 11 shows the life predictions compared to the experimental results for the different flaw sizes. The flow stress used in these predictions was calculated using the 0.2% offset yield stress and the ultimate tensile strength for the titanium. At the lower stress levels the predictions for an initial  $6 \mu\text{m}$  flaw are within a factor of two of the experimental results. At the higher stresses the results deviate greatly, by about an order of magnitude. At these stresses, a large amount of plastic deformation occurs and the crack tip plastic zone may encompass the net section

more rapidly than the model predicts, resulting in longer life predictions. When the flow stress was calculated using the proportional limit stress and the ultimate tensile strength, the plasticity correction had a greater effect. Figure 12 compares the life predictions for a 6  $\mu\text{m}$  initial flaw as a function of flow stress. This flaw size was consistent with previous studies predicting the fatigue life of titanium alloys having an acicular alpha phase present in the microstructure [10]. Using the lower flow stress resulted in under predicted lives at the higher stress levels. At the lower stress levels, predictions correlate better with the experimental results. The predictions using the two flow stresses appear to bound the experimental data at the higher stress levels. Deviations by predictions from the experimental results may be attributed to the complexity of the material and the perforation geometry. The combination of the conical holes with irregular surfaces may affect the stress concentration factor and initially raise the local stresses that cause yielding. Throughout the analysis a stress concentration factor of  $K_t=3$  was assumed; the irregular holes may produce a greater stress concentration effect. Other changes in the nature of the titanium due to the laser-drilling process may add further complications. In the region of the perforation the titanium composition may have changed during the laser drilling due to the infusion of oxygen into the material. This oxygen rich surface layer at the hole boundary would then be more brittle than the remaining material and would be expected to influence the fatigue behavior. In general, the elastic-plastic analysis did show the general trends of the fatigue behavior of the perforated titanium, although further analysis of the stress concentration effect of the hole and the compositional changes in the material may give better life predictions.

### **Concluding Remarks**

Laminar flow control (LCF) offers improved aerodynamic efficiency to aircraft by reducing drag and subsequently allowing for increased range and load capacity. A proposed method of implementing LCF involves reducing the boundary layer on some areas of the wings by applying suction through small perforations in the skin. The objectives of this study were to investigate the influence of multiple perforations on the fatigue behavior of commercially pure titanium and to predict the fatigue life of the perforated material using an elastic-plastic crack closure model. Room

temperature tension tests were conducted to characterize the material's mechanical properties in addition to the room temperature constant amplitude fatigue tests. To establish a baseline for comparison, non-perforated sheets were also tested in tension and fatigue. A two dimensional finite element analysis was used to determine that the stress fields from adjacent perforations did not influence one another. Fatigue crack growth tests were conducted to provide input to the crack closure model. Life predictions were made using an equivalent initial flaw size approach to relate the experimental constant amplitude fatigue test results to the microstructural features of the titanium.

Test results showed the multiple perforations did not affect the tensile response, but did reduce the fatigue life. The stress analysis determined that the stress fields around the holes do not overlap one another, allowing the material to be modeled as a plate with a center hole in life prediction calculations. Predictions using flaw sizes ranging from 1 to 15  $\mu\text{m}$  correlated within a factor of 2 with the experimental results. By using two different flow stresses in the crack closure model and correcting for plasticity, the experimental results were bounded by the predictions at the higher stress levels. Further analysis of the complex geometry of the perforations and the local material chemistry is needed to further understand the fatigue behavior of the perforated titanium.

### **Acknowledgments**

The first author acknowledges the support extended by the National Research Council (NRC), Washington, D.C. through its associateship program.

### **References**

1. Harris, R.V and Hefner, J.N., "NASA Laminar Flow Program--Past, Present and Future," Research in Natural Laminar Flow and Laminar Flow Control, Part I, NASA Langley Research Center, 1987, pp. 25-44.
2. Morris, J., "LFC-- A Maturing Concept," Research in Natural Laminar Flow and Laminar Flow Control, Part I, NASA Langley Research Center, 1987, pp. 45-51.
3. ASM International, Metals Handbook, Eighth Edition, Vol. 2, pp. 593-594.

4. ASTM, Annual Book of ASTM Standards, Vol. 3.01, E647-93, 1994, pp. 569-647.
5. Wawrzynek, P.A. and Ingraffea, A.R., "Interactive Finite Element Analysis of Fracture Processes: An Integrated Approach," Theoretical and Applied Fracture Mechanics, Vol. 8, 1987, pp. 137-150.
6. Newman, J.C., Jr., "FASTRAN-II--A Fatigue Crack Growth Structural Analysis Program," NASA Technical Memorandum 104159, February 1992.
7. Suresh, S., Fatigue of Materials, Cambridge University Press, Cambridge, 1991, pp. 272-290.
8. Newman, J.C., Jr., "A Crack-Opening Stress Equation for Fatigue Crack Growth," International Journal of Fracture, Vol. 24, 1984, pp. R131-R135.
9. Newman, J.C., Jr., Phillips, E.P., and Everett, R.A., Jr., "Fatigue Life and Crack Growth Prediction Methodology," NASA Technical Memorandum 109044, October 1993.
10. Newman, J.C., Jr., Phillips, E.P., Swain, M.H., and Everett, R.A., Jr., "Fatigue Mechanics: An Assessment of a Unified Approach to Life Prediction," Advances in Fatigue Lifetime Predictive Techniques, ASTM STP 1122, M.R. Mitchell and R.W. Landgraf, EDs., American Society for Testing and Materials, Philadelphia, 1992, pp. 5-27.

Table 1. Chemical composition of commercially pure titanium (weight percent)

N	C	H	Fe	O	Pd
0.005	0.008	0.0023	0.033	0.060	0.003

Table 2. Tensile mechanical properties of non-perforated and perforated commercially pure titanium

	Non-Perforated	Perforated
Gross Elastic Modulus, GPa	105	95
Net Elastic Modulus, GPa	105	105
Proportional Limit Stress, MPa	152	138
0.2% Offset Yield Stress, MPa	275	275
Ultimate Strength, MPa	386	393
% Elongation	14.0	13.7

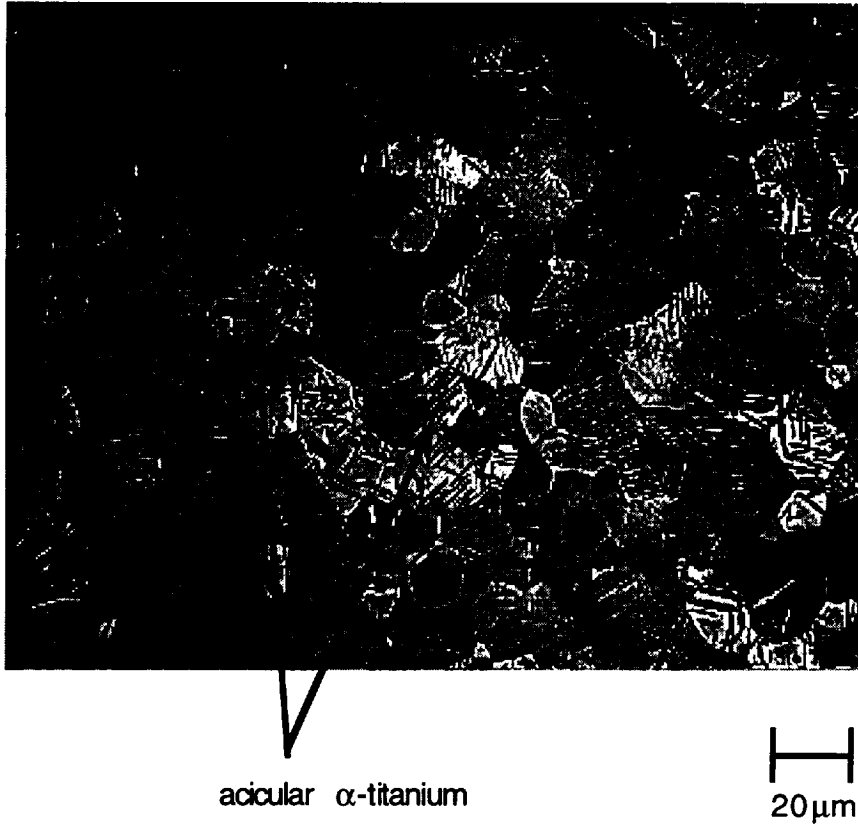


Figure 1. Microstructure of commercially pure titanium.

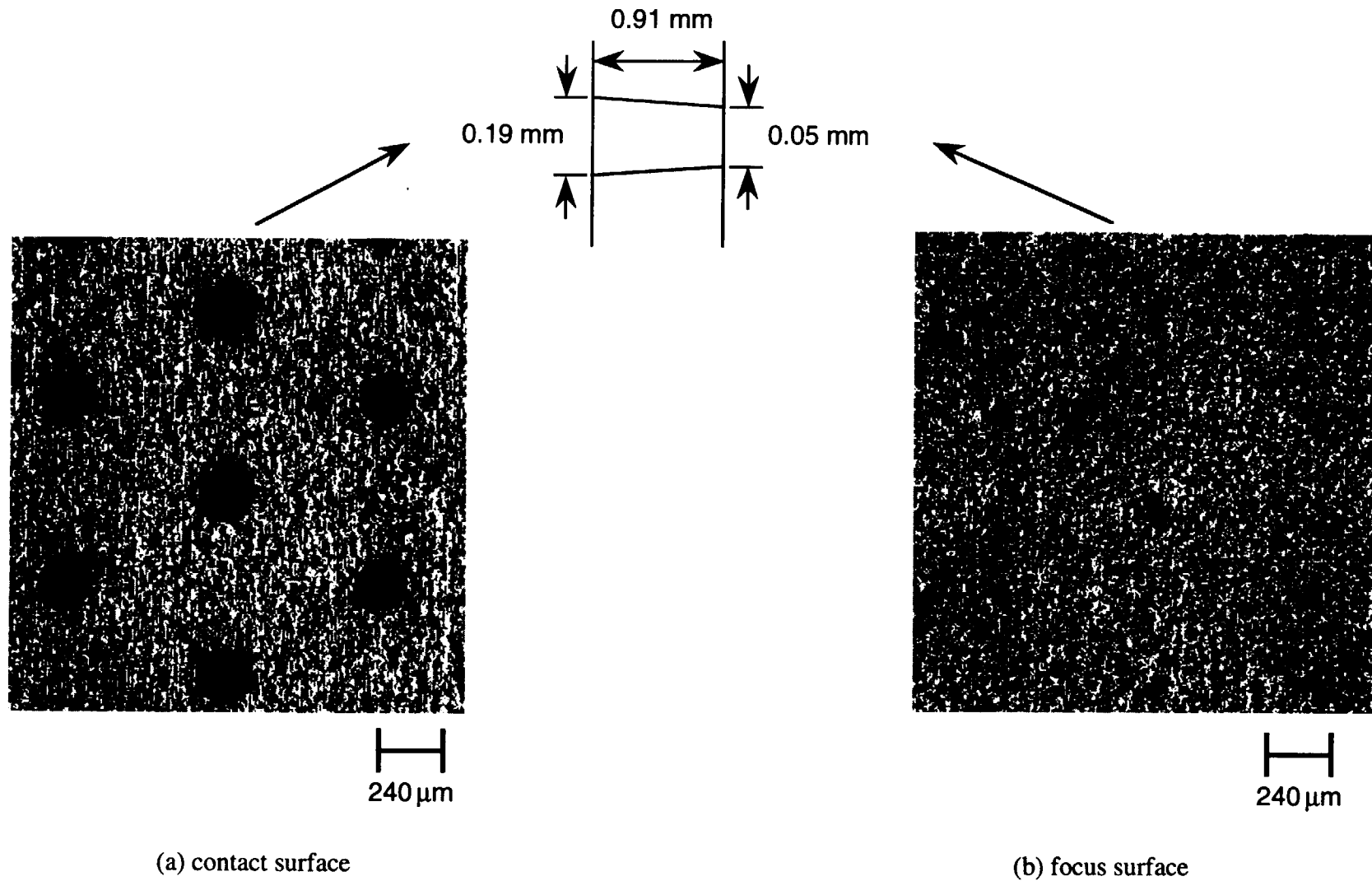
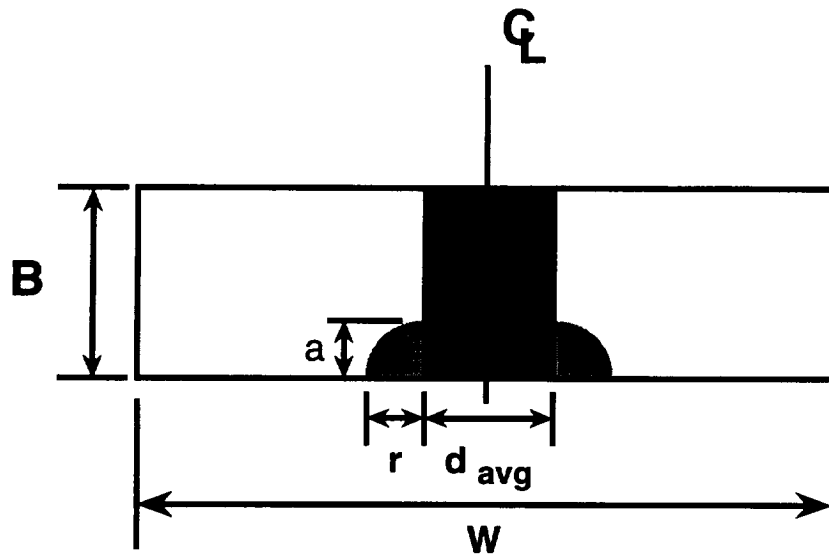
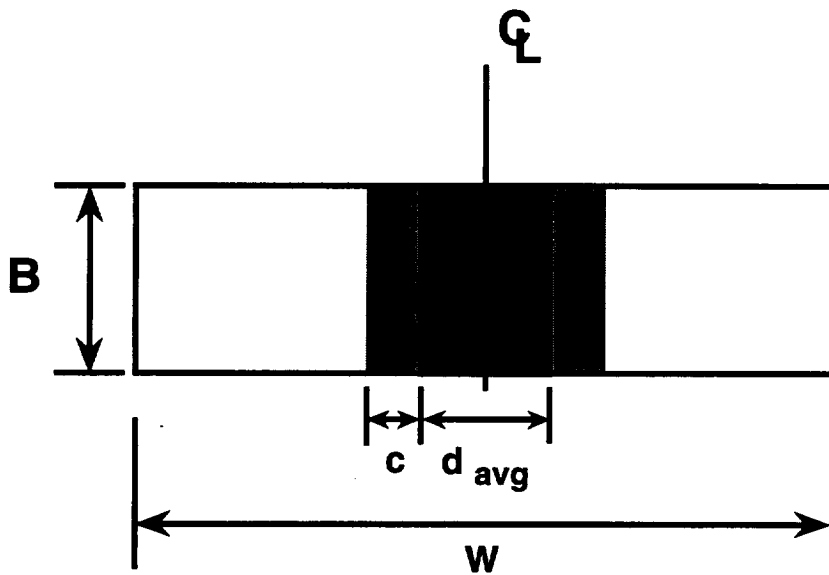


Figure 2. Surfaces of perforated titanium sheets after laser drilling: a) larger hole diameter corresponds to first surface cut by the laser; b) smaller hole diameter corresponds to the focus point of the laser.



(a) corner-crack configuration



(b) through-crack configuration

Figure 3. Schematic diagrams of specimen cross sections showing crack configurations used for determining boundary correction factors: a) corner-crack configuration and b) through-crack configuration.

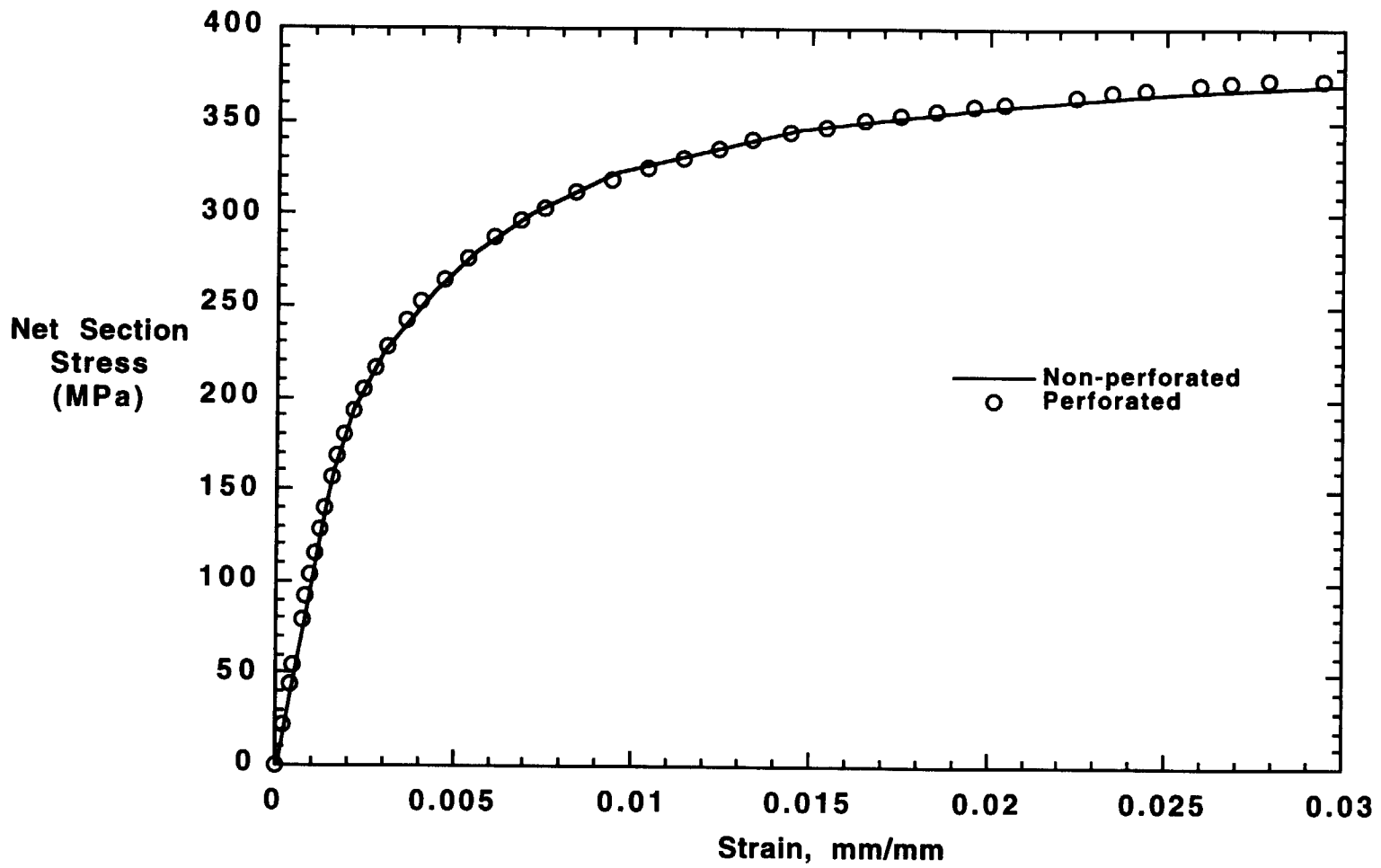


Figure 4. Tensile response of non-perforated and perforated commercially pure titanium.

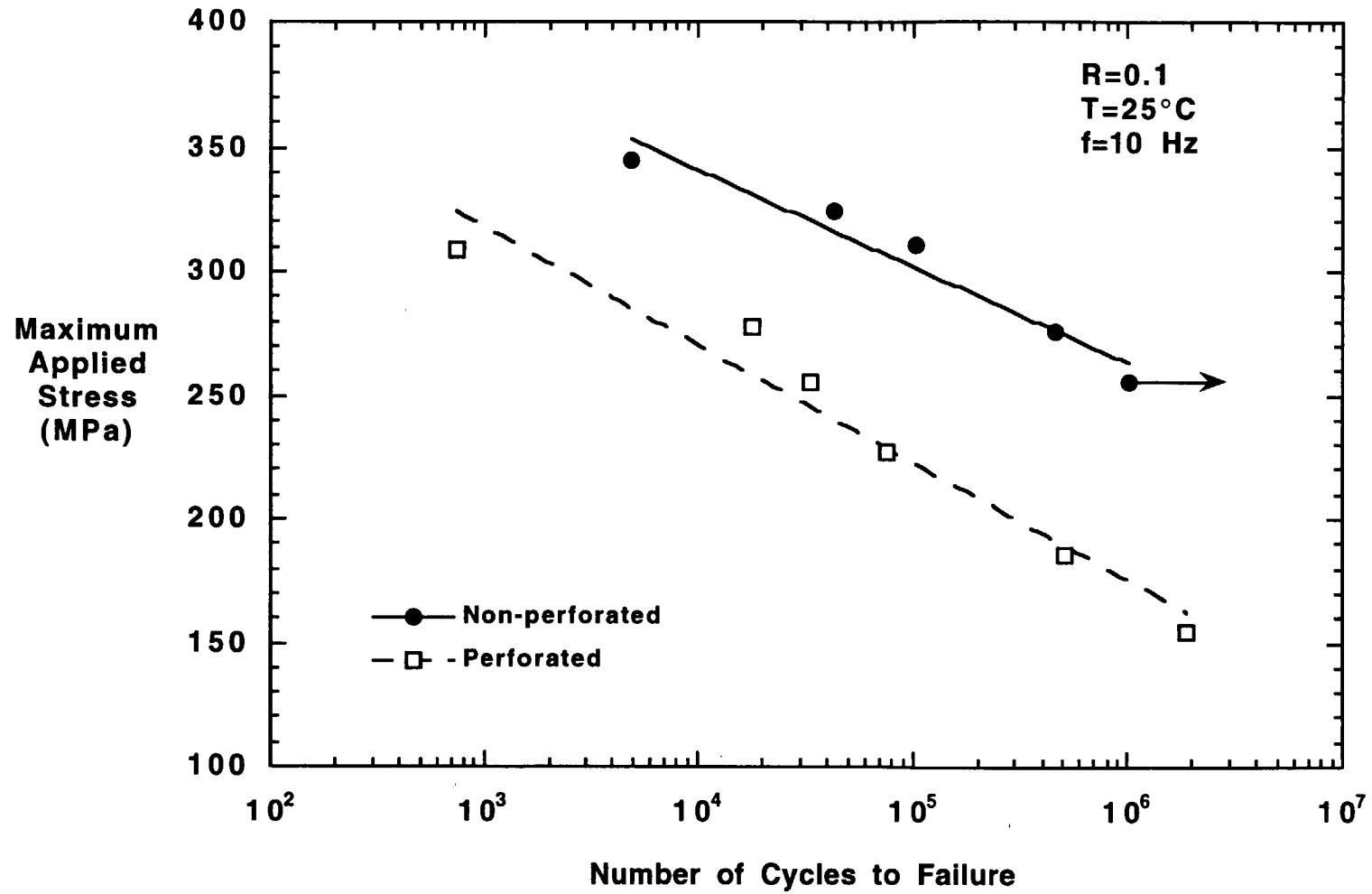


Figure 5. Maximum applied stress versus number of cycles to failure for non-perforated and perforated commercially pure titanium subjected to constant amplitude fatigue.

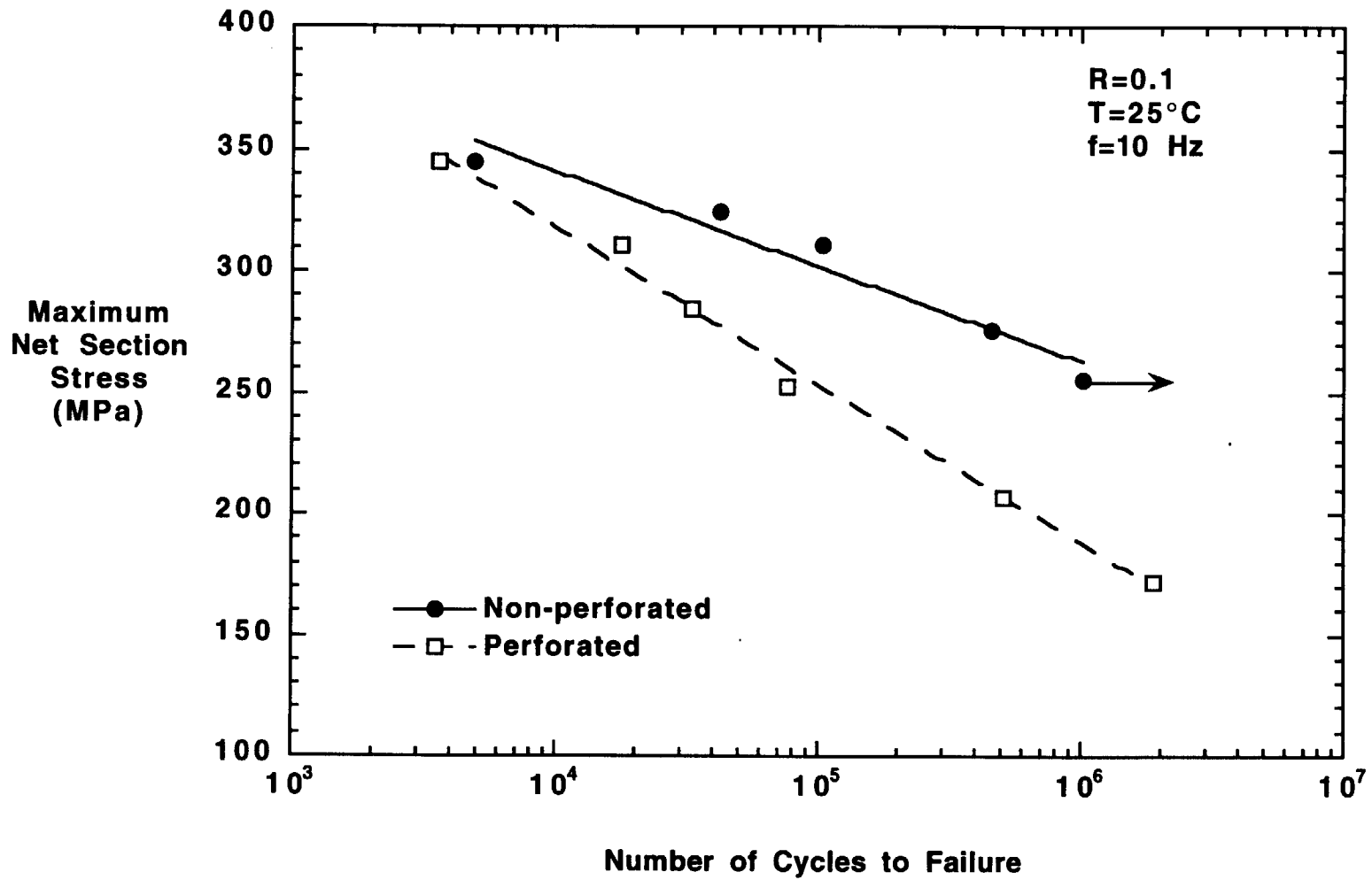
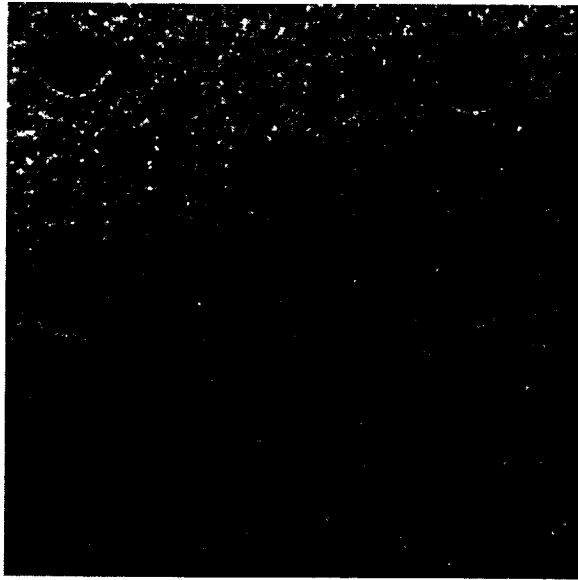
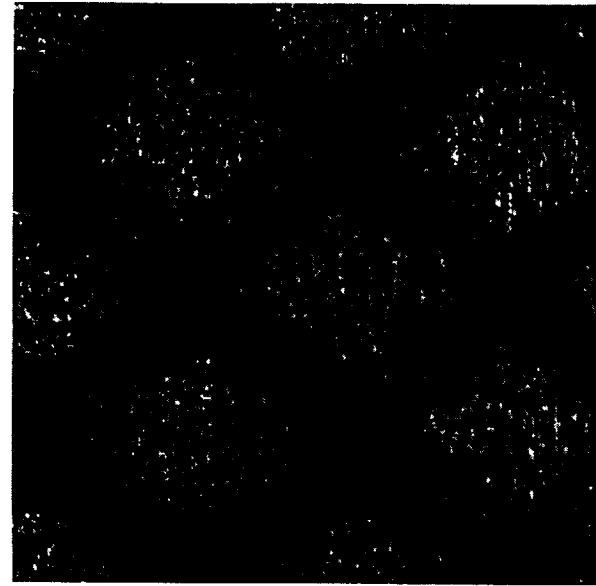


Figure 6. Maximum net section stress versus number of cycles to failure for non-perforated and perforated commercially pure titanium subjected to constant amplitude fatigue.



200  $\mu$  m

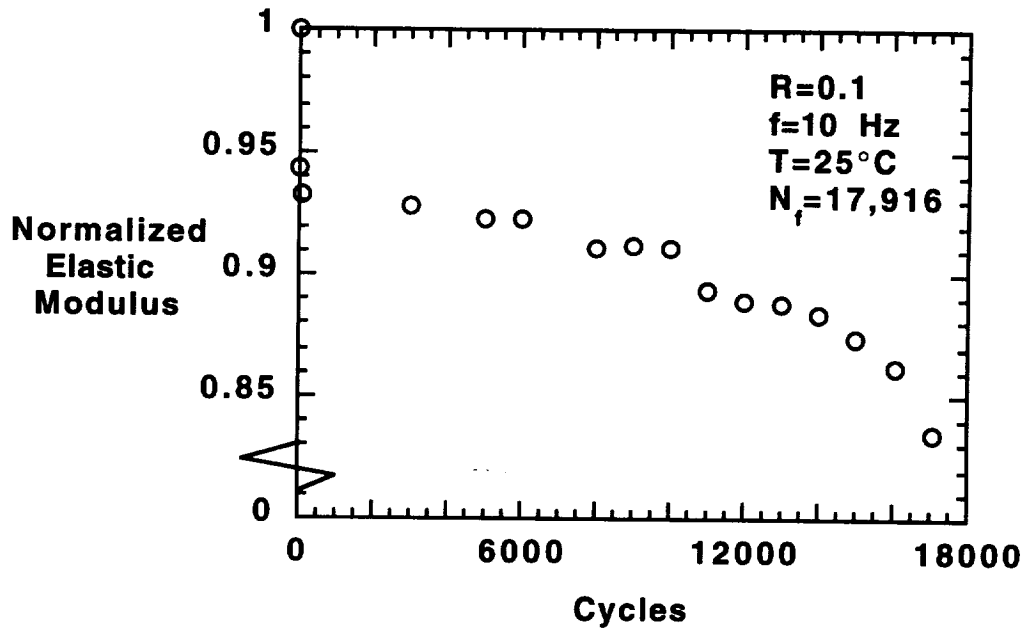
(a) 227 MPa applied stress



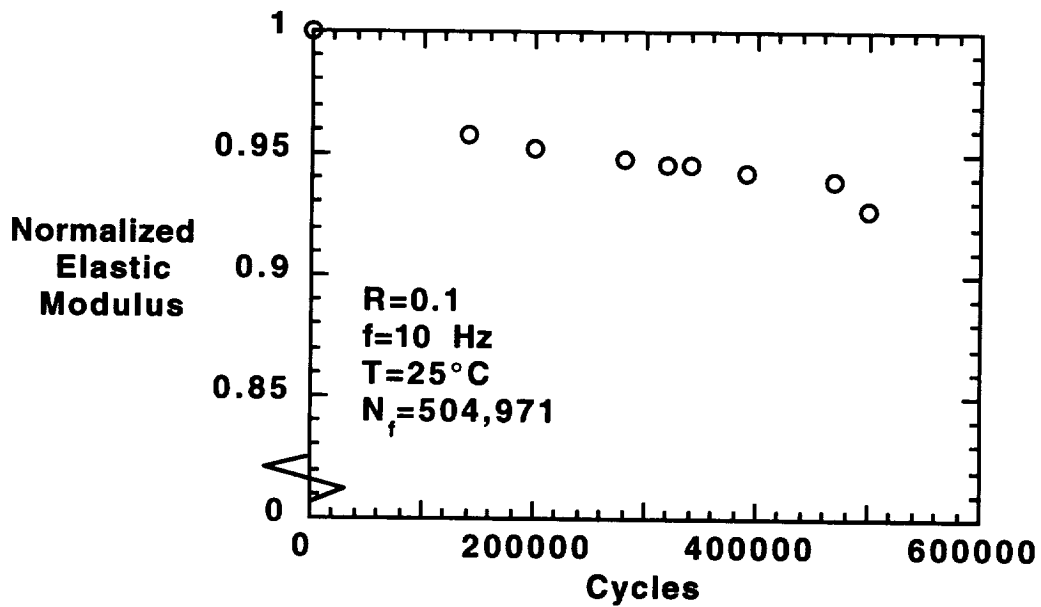
200  $\mu$  m

(b) 345 MPa applied stress

Figure 7. Surfaces of perforated titanium specimens after being subjected to constant amplitude fatigue tests: a) 227 MPa applied stress and b) 345 MPa applied stress.



(a) 276 MPa applied stress



(b) 186 MPa applied stress

Figure 8. Reduction in normalized elastic modulus during constant amplitude fatigue of perforated commercially pure titanium: a) at 276 MPa applied stress; b) at 186 MPa applied stress.

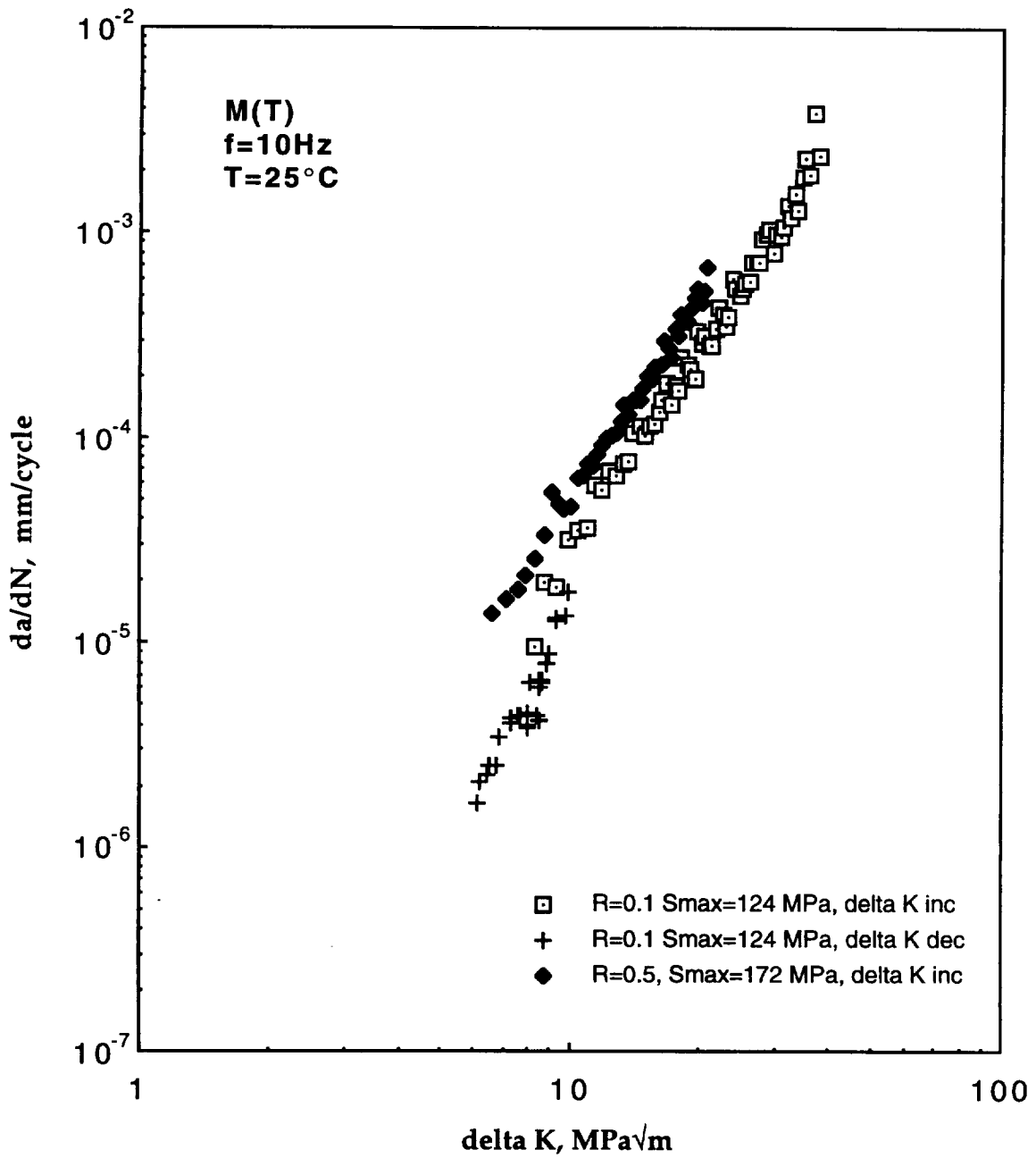


Figure 9. Fatigue crack growth rate vs.  $\Delta K$  for commercially pure titanium at  $R=0.1$  and  $0.5$ .

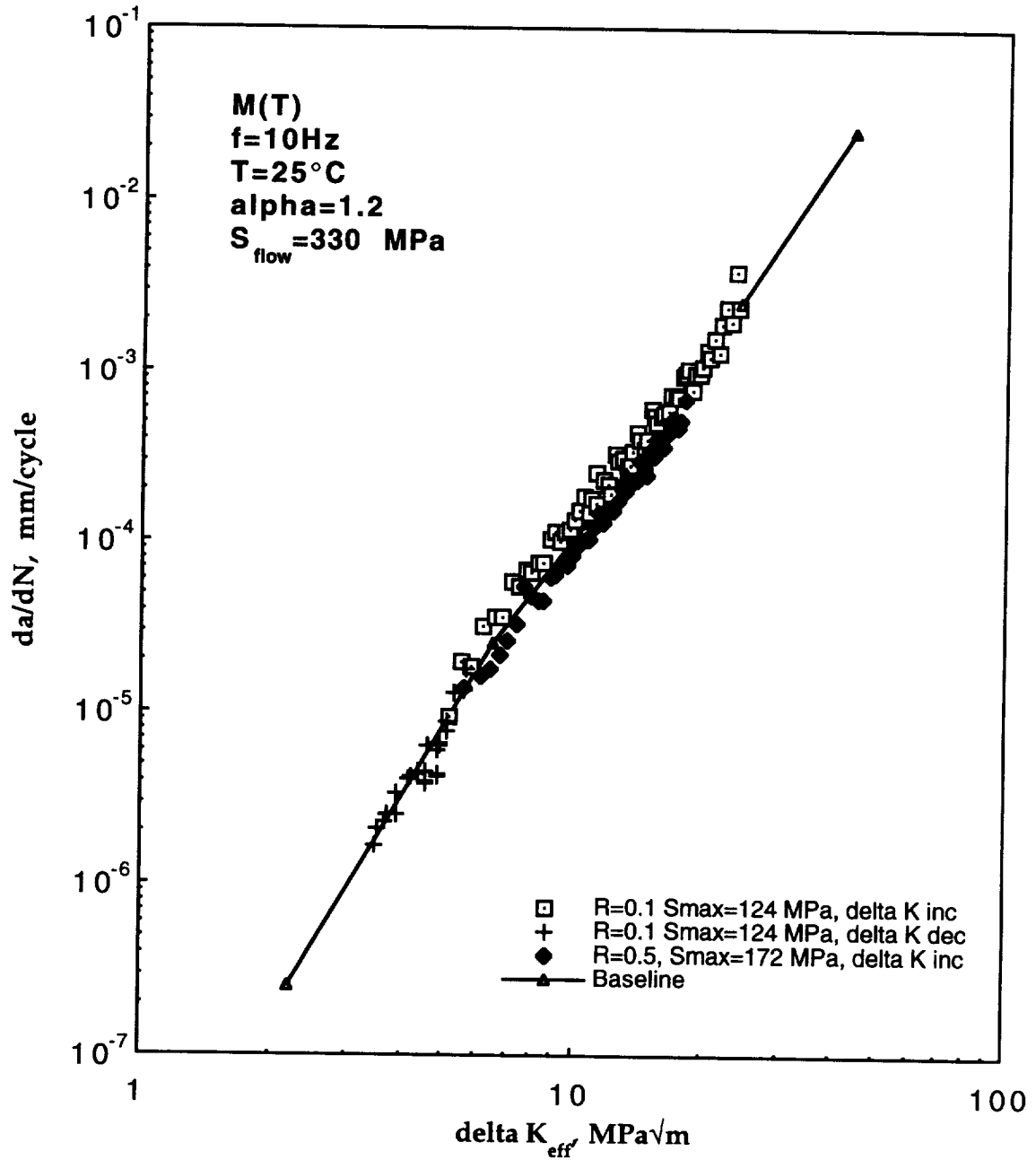


Figure 10. Fatigue crack growth rate vs.  $\Delta K_{eff}$  for commercially pure titanium at  $R=0.1$  and  $0.5$ .

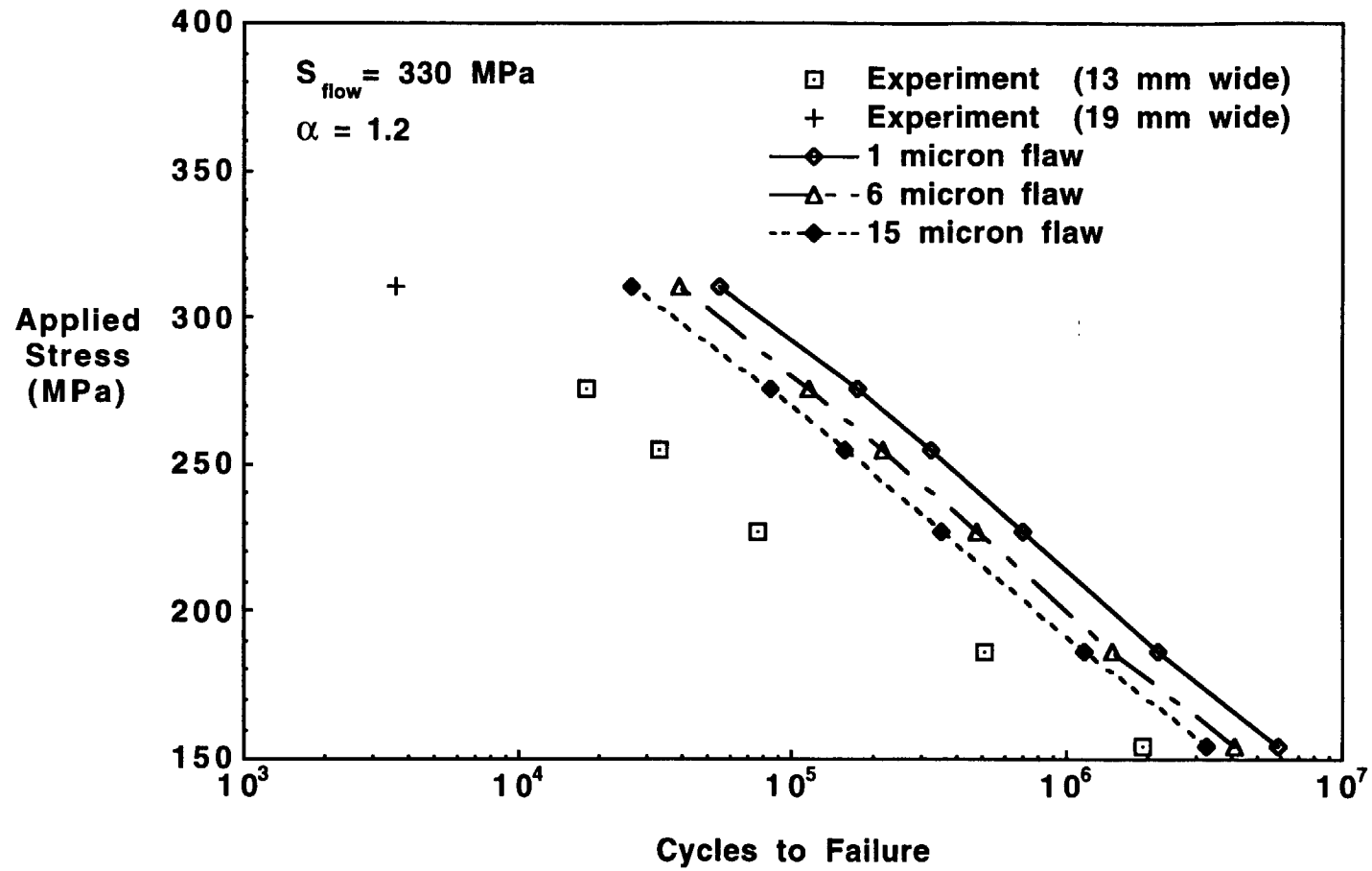


Figure 11. Experimental and predicted fatigue life for perforated commercially pure titanium at  $R=0.1$  using various initial flaw sizes.

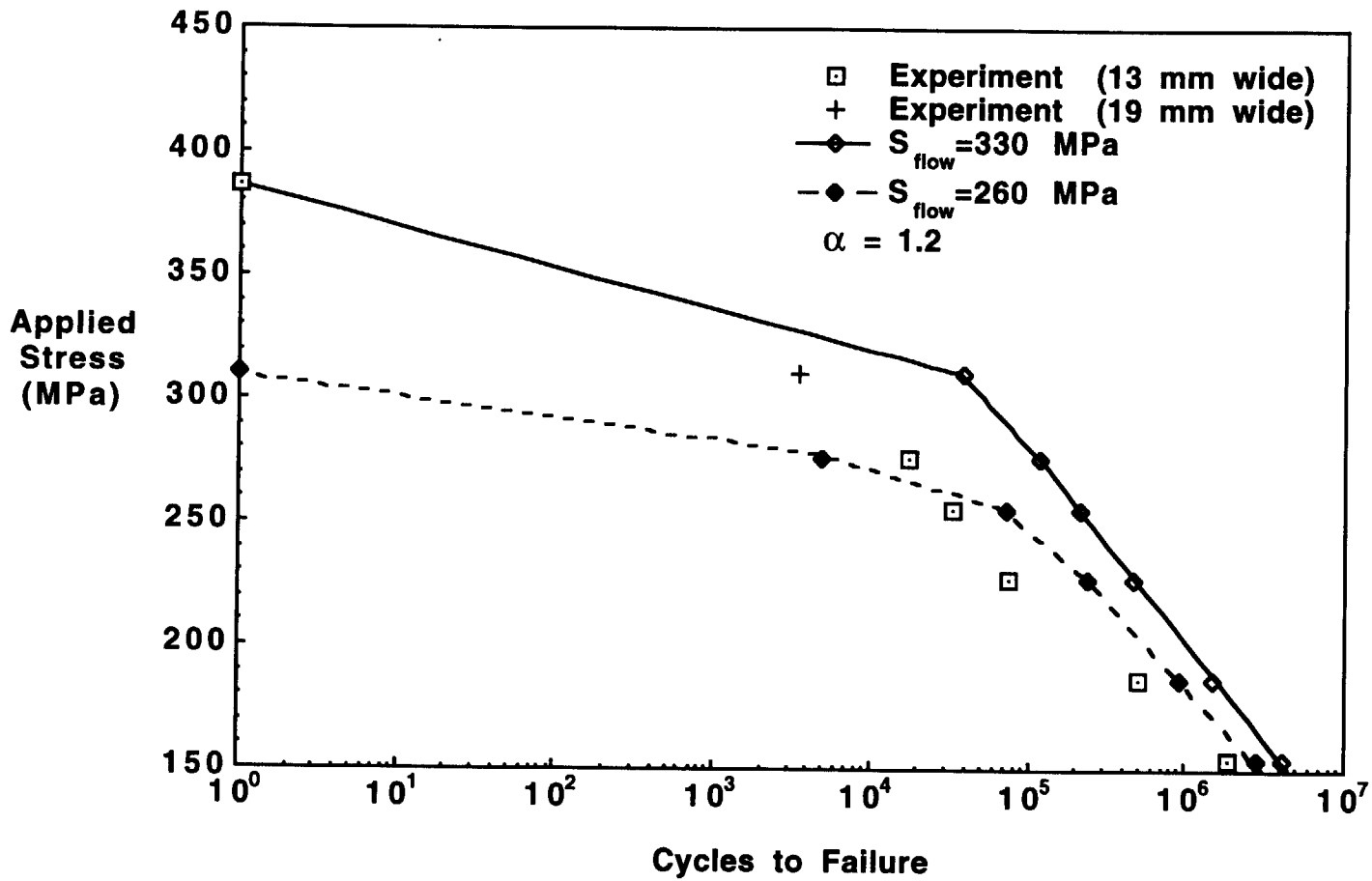


Figure 12. Experimental and predicted fatigue life for perforated commercially pure titanium at  $R=0.1$  using different flow stresses.

## APPENDIX A - Finite Element Analysis

An elastic finite element stress analysis was conducted using FRANC2D [5] to determine whether the stress fields from the holes interact. As a comparison, a large plate with a central hole was also analyzed. The finite element meshes were generated using the CASCA mesh generator and are shown in Figure A1. The perforated titanium sheet was modeled using six-noded triangular isoparametric elements while the large plate with a central hole used six-noded triangles in the refined region surrounding the hole and 8-noded quadrilateral elements in the coarse far field region. A linear elastic analysis was conducted by applying a uniform stress  $\sigma_{yy}=S$  on  $y=b$  as in Figure A1.

The stress contours were generated for both the perforated titanium model and the large plate with a center hole model. A comparison of the  $\sigma_{yy}$  stress contours for the two cases is shown in Figure A3. The elastic stress concentration factor is 3.10 for the perforated titanium sheet model and 3.06 for the large plate with a central hole, resulting in a similar stress field near the holes. In the ligament between the holes, the stresses are comparable to the far field stresses in the large plate. The stress fields around the holes did not influence one another and thus can be treated as acting independent of one another. The stress analysis agrees with the visual evidence of the cracking of the specimens tested at the lower stress levels, as previously mentioned, where the cracks appeared to grow along straight paths from the holes. At the higher stresses where more plastic deformation was shown, shear bands developed linking the holes (Figure 6b). The shear bands develop in the region of maximum shear stress as indicated by the shear stress contours in Figure A4. Because the stress analysis showed the perforated titanium resembled an large plate with a central hole, this configuration was chosen for the life prediction model. The geometry of the specimen used for the life prediction model was determined from the periodic array spacing of the perforations. The specimen width was set equal to the center-to-center spacing of the perforations in the crack growth direction and the center hole size was set to equal the average perforation diameter.

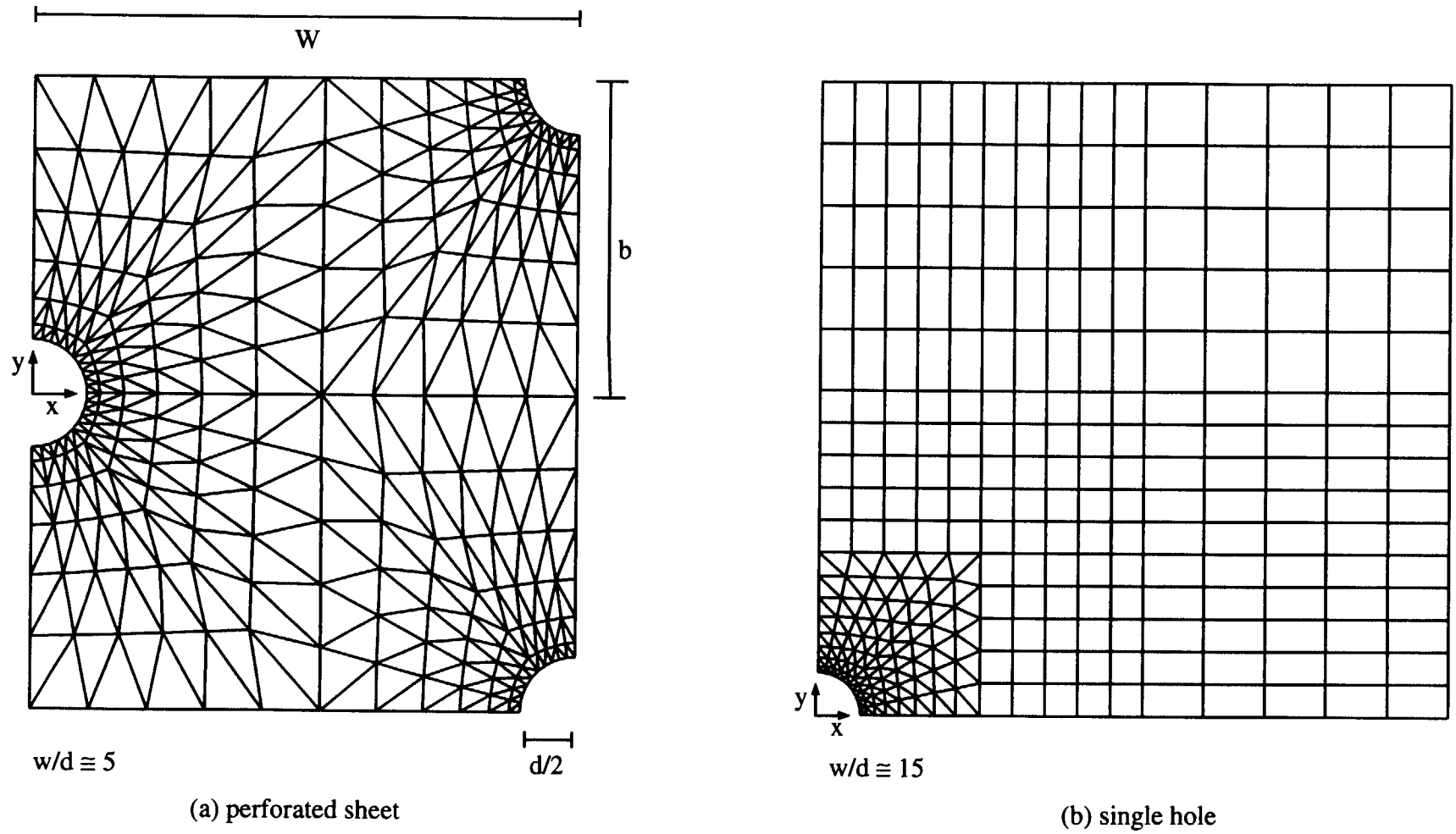


Figure A1. Finite element models for: a) perforated sheet b) large plate with a central hole.

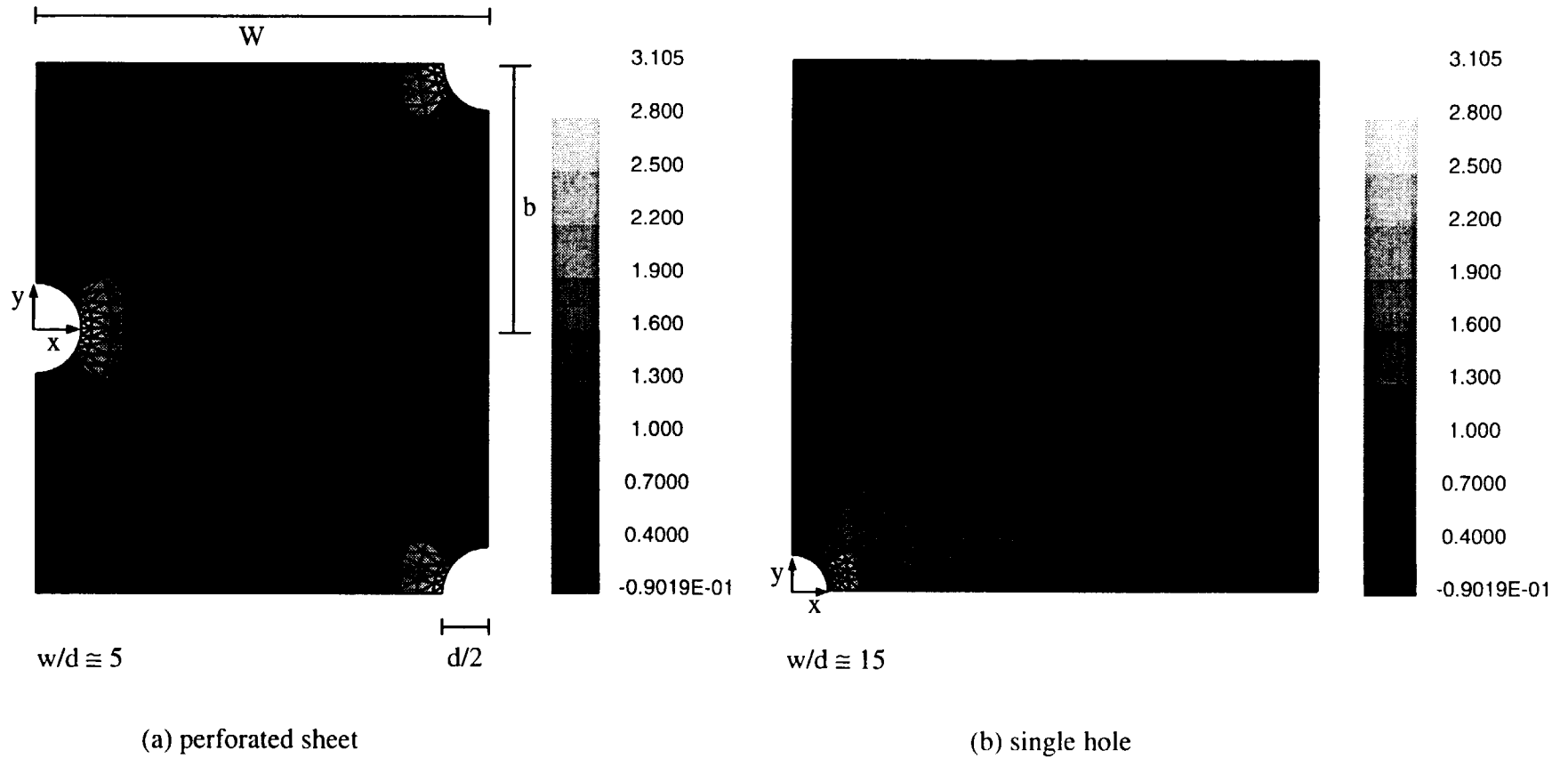


Figure A2. Comparison of stress contours ( $\sigma_{yy}$ ) from finite element analysis: a) unit cell representation of the perforated titanium specimen; b) large plate with a central hole.

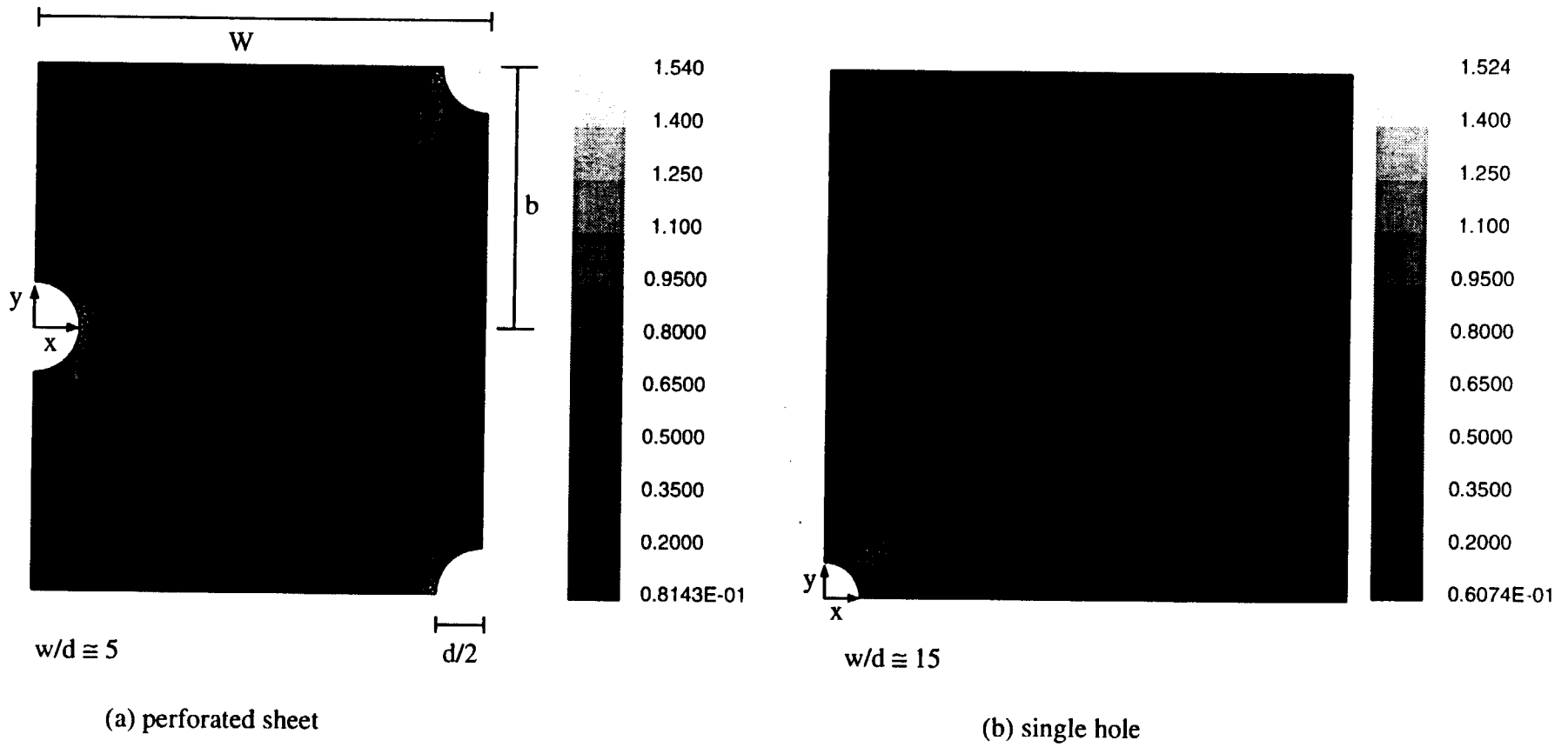


Figure A3. Comparison of the maximum shear stress contours from finite element analysis: a) unit cell representation of the perforated titanium specimen; b) large plate with a central hole.



# REPORT DOCUMENTATION PAGE

*Form Approved*  
*OMB No. 0704-0188*

Public reporting burden for this collection of information is estimated to average 1 hour per response, including the time for reviewing instructions, searching existing data sources, gathering and maintaining the data needed, and completing and reviewing the collection of information. Send comments regarding this burden estimate or any other aspect of this collection of information, including suggestions for reducing this burden, to Washington Headquarters Services, Directorate for Information Operations and Reports, 1215 Jefferson Davis Highway, Suite 1204, Arlington, VA 22202-4302, and to the Office of Management and Budget, Paperwork Reduction Project (0704-0188), Washington, DC 20503.

<b>1. AGENCY USE ONLY (Leave blank)</b>		<b>2. REPORT DATE</b> April 1996	<b>3. REPORT TYPE AND DATES COVERED</b> Technical Memorandum	
<b>4. TITLE AND SUBTITLE</b> Fatigue Response of Perforated Titanium for Application in Laminar Flow Control			<b>5. FUNDING NUMBERS</b> WU 538-02-10-01	
<b>6. AUTHOR(S)</b> Jennifer L. Miller, James C. Newman, Jr., and W. Steven Johnson				
<b>7. PERFORMING ORGANIZATION NAME(S) AND ADDRESS(ES)</b> NASA Langley Research Center Hampton, VA 23681-0001			<b>8. PERFORMING ORGANIZATION REPORT NUMBER</b>	
<b>9. SPONSORING / MONITORING AGENCY NAME(S) AND ADDRESS(ES)</b> National Aeronautics and Space Administration Washington, DC 20546-0001			<b>10. SPONSORING / MONITORING AGENCY REPORT NUMBER</b>  NASA TM-110251	
<b>11. SUPPLEMENTARY NOTES</b> Miller, Resident Research Associate for the National Research Council, and Newman, Jr.: Langley Research Center, Hampton, VA; Johnson: Georgia Institute of Technology, Atlanta, GA.				
<b>12a. DISTRIBUTION / AVAILABILITY STATEMENT</b>  Unclassified - Unlimited  Subject Category 24			<b>12b. DISTRIBUTION CODE</b>	
<b>13. ABSTRACT (Maximum 200 words)</b>  The room temperature tensile and fatigue response of non-perforated and perforated titanium for laminar flow control application was investigated both experimentally and analytically. Results showed that multiple perforations did not affect the tensile response, but did reduce the fatigue life. A two dimensional finite element stress analysis was used to determine that the stress fields from adjacent perforations did not influence one another. The stress fields around the holes did not overlap one another, allowing the materials to be modeled as a plate with a center hole. Fatigue life was predicted using an equivalent initial flow size approach to relate the experimental results to microstructural features of the titanium. Predictions using flaw sizes ranging from 1 to 15 $\mu\text{m}$ correlated within a factor of 2 with the experimental results by using a flow stress of 260 MPa. By using two different flow stresses in the crack closure model and correcting for plasticity, the experimental results were bounded by the predictions for high applied stresses. Further analysis of the complex geometry of the perforations and the local material chemistry is needed to further understand the fatigue behavior of the perforated titanium.				
<b>14. SUBJECT TERMS</b> Commercially pure titanium; Tensile response; Fatigue crack growth; Life prediction; Cracks			<b>15. NUMBER OF PAGES</b> 29	
			<b>16. PRICE CODE</b> A03	
<b>17. SECURITY CLASSIFICATION OF REPORT</b> Unclassified	<b>18. SECURITY CLASSIFICATION OF THIS PAGE</b> Unclassified	<b>19. SECURITY CLASSIFICATION OF ABSTRACT</b>	<b>20. LIMITATION OF ABSTRACT</b>	



